# Effect of the Ca content on the electronic structure of Pb 1x Ca x TiO 3 perovskites

J. C. Jan, K. P. Krishna Kumar, J. W. Chiou, H. M. Tsai, H. L. Shih, H. C. Hsueh, S. C. Ray, K. Asokan, W. F. Pong, M.-H. Tsai, S. Y. Kuo, and W. F. Hsieh

---

**Articles you may be interested in**

An ab-initio DFT study of electronic structure of SrMO 3 perovskites (M = Rh and Ru)
AIP Conf. Proc. **1536**, 1077 (2013); 10.1063/1.4810608

Effects of strain on the electronic structures and T C 's of the La 0.67 Ca 0.33 Mn O 3 and La 0.8 Ba 0.2 Mn O 3 thin films deposited on Sr Ti O 3
Appl. Phys. Lett. **89**, 082511 (2006); 10.1063/1.2335973

Electronic structure of Pb 1  x La x Ti O 3 ferroelectric materials from Ti 2 p and O 1 s soft x-ray absorption spectroscopy
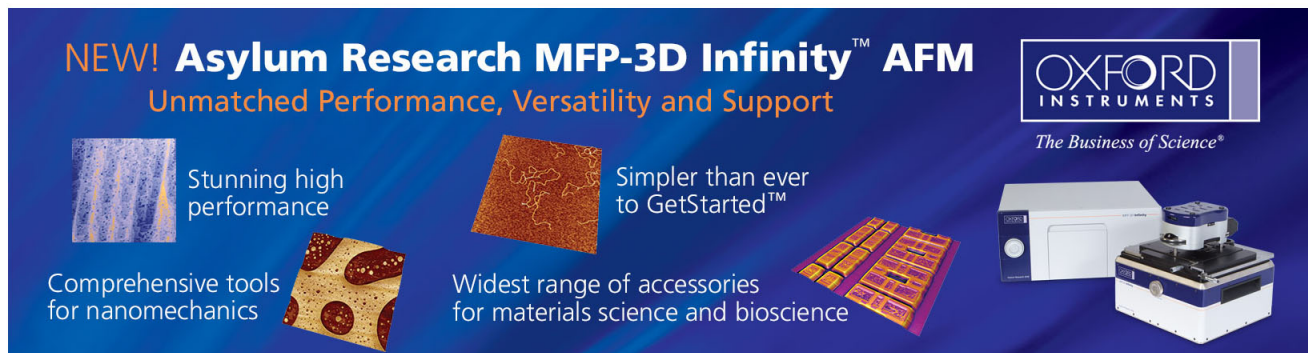J. Appl. Phys. **99**, 044104 (2006); 10.1063/1.2173683

Direct experimental evidence of hybridization of Pb states with O 2 p states in ferroelectric perovskite oxides
Appl. Phys. Lett. **87**, 012103 (2005); 10.1063/1.1988984

Prediction of the [Na 1/2 Bi 1/2 ]TiO 3 ground state
AIP Conf. Proc. **582**, 82 (2001); 10.1063/1.1399692

---

# Effect of the Ca content on the electronic structure of $Pb_{1-x}Ca_xTiO_3$ perovskites

J. C. Jan, K. P. Krishna Kumar, J. W. Chiou, H. M. Tsai, H. L. Shih, H. C. Hsueh, S. C. Ray, K. Asokan,[a] and W. F. Pong[b]
*Department of Physics, Tamkang University, Tamsui, Taiwan 251, Republic of China*

M.-H. Tsai
*Department of Physics, National Sun Yat-Sen University, Kaohsiung, Taiwan 804, Republic of China*

S. Y. Kuo[c] and W. F. Hsieh
*Institute of Electro-Optical Engineering, National Chiao Tung University, Hsinchu, Taiwan 300, Republic of China*

This study performs O $K$- and Ti $L_{3,2}$-edge x-ray absorption near-edge structure (XANES) measurements and first-principles pseudopotential calculations for the electronic structures of $ABO_3$-type $Pb_{1-x}Ca_xTiO_3$ ($x=0-1$) perovskites. The features in the O $K$-edge XANES spectra are found to be contributed primarily by hybridization between O $2p$ and Ti $3d$, Pb $6p$, and Ca $3d$ orbitals. The O $K$-edge XANES spectra reveal that partial substitution of A cations, Pb, by Ca not only decreases O $2p$–Pb $6p$ but also O $2p$–Ti $3d$ hybridization. The Ti $L_{3,2}$-edge measurements find that the off-center displacement of Ti, and hence, ferroelectricity persist up to a Ca concentration between 0.3 and 0.4. © *2003 American Institute of Physics.*
[DOI: 10.1063/1.1618375]

Ferroelectric $ABO_3$ perovskites have been the subject of extensive studies since they exhibit rich electric characteristics potentially useful in fundamental research and technological applications.[1] Among them lead titanate, $PbTiO_3$ (denoted as PTO) has a characteristic unit cell that contains a highly polarizable $TiO_6$ octahedron, which gives rise to ferroelectric characteristics.[1,2] Theoretical calculations showed that Ti $3d$ and O $2p$ hybridized states and the Pb–O covalent bonding crucially cause the ferroelectric instability in PTO.[3–5] While previous extended x-ray absorption fine structure studies of ferroelectric titanates revealed the off-center displacement of Ti.[6] Introducing Ca was found to reduce both the tetragonal distortion and the transition temperature of PTO.[7] Recently, compositional substitution of the A cation, Pb, in PTO by Ca and the effect on its electrical and structural characteristics have been studied by x-ray diffraction and Raman measurements.[8,9] The x-ray diffraction measurement performed by Kuo *et al.* showed that as the Ca content in $Pb_{1-x}Ca_xTiO_3$ ($PC_xTO$) increased from 0 to 1, phase transitions from tetragonal to cubic and then to orthorhombic occurred.[9] In this study, O $K$- and Ti $L_{3,2}$-edge x-ray absorption near-edge structure (XANES) measurements and first-principles electronic structure calculations[10] are performed to better understand the influence of Ca substitution on the electronic structure of $PC_xTO$ perovskites.

Room temperature XANES spectra at O $K$ and Ti $L_{3,2}$ edges were obtained using a high-energy spherical grating monochromator beamline by the fluorescence and sample

current modes, respectively, at the National Synchrotron Radiation Research Center, Hsinchu, Taiwan. Powdered $PC_xTO$ samples were synthesized using the sol-gel technique. Theoretical calculations of $Pb_{0.5}Ca_{0.5}TiO_3$ were based on the first-principles pseudopotential method with the local-density approximation,[11] the computation details are given elsewhere.[10,12]

Figure 1 presents the O $K$-edge XANES spectra of $PC_xTO$ ($x=0.2-0.9$), $PbTiO_3$ ($x=0$, PTO), $CaTiO_3$ ($x=1$, CTO) and the reference $TiO_2$. These spectra are normalized to the same area in the energy range between 550 and 570 eV (not fully shown). The features marked by $A_1$ to $D_1$ in the spectra of $PC_xTO$ and $TiO_2$ are centered at $\sim$530.8, 532.4, 533.6, and 536.0 eV, respectively. The inset in Fig. 1 presents a magnified view to better resolve features $A_1-D_1$. In these spectra, the background intensity was subtracted from a best-fitted Gaussian curve as indicated by the dashed lines. These features are best resolved with two peaks for CTO and $TiO_2$. Similar two-peak structures at the threshold of the O $K$ edge were also observed for other $3d$-transition metal oxides.[13] The two-peak structures, marked by $A_1$ and $C_1$, in the CTO and $TiO_2$ spectra, are contributed by O $2p$ and Ti $t_{2g}$ and $e_g$ antibonding orbitals, respectively.[12,13]

Figure 2 shows the O $K$-edge XANES spectrum and the calculated O $2p$-, Ti $3d$-, Pb $6sp$-, and Ca $3d$-derived states of the $Pb_{0.5}Ca_{0.5}TiO_3$ to elucidate O $2p$–Ti $3d$, O $2p$–Pb $6sp$, and O $2p$–Ca $3d$ hybridization and to identify the contributions to the O $K$-edge XANES features. Figure 2 reveals strong hybridization between O $2p$ and Ti $3d$ $t_{2g}$ and $e_g$ orbitals, which gives rise to features $A_1$ and $C_1$, respectively. Features $B_1$ and $D_1$ arise predominantly from the hybridization between O $2p$ and Pb $6p$ and Ca $3d$ orbitals, respectively.
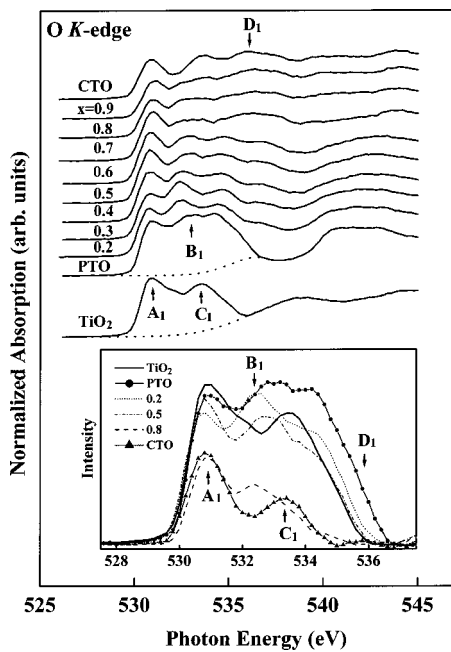
Figure 3 presents the difference curves of the O $K$-edge

FIG. 1. Normalized O $K$-edge XANES spectra of the PC$_x$TO ($x=0-1$) samples. The dashed line represents a best-fitted Gaussian shape background. The inset shows the magnified near-edge feature after the background subtraction.

XANES spectra of PC$_x$TO and PTO to illustrate the dependence of the hybridization between O $2p$ and Ti $3d$, Pb $6p$ and Ca $3d$ orbitals on $x$. The darkened areas under the difference curve (hereafter denoted as $\Delta A_1$, $\Delta B_1$, $\Delta C_1$, and $\Delta D_1$) are proportional to the difference between the densities of the unoccupied O $2p$-derived states of PC$_x$TO and those of PTO. Figure 3 reveals that the areas under $\Delta A_1$ to $\Delta C_1$ ($\Delta D_1$) are always negative (positive) and increase with the Ca content, indicating reduced (increased) O $2p$–Ti $3d$ and O $2p$–Pb $6p$ (O $2p$–Ca $3d$) hybridization with the Ca substitution. Roughly three different regions can be identified for $x$ between 0 and 0.3, 0.4, and 0.6, and 0.7 and 1 according to the variation of the intensities and line shapes of the difference spectra. The trend of the line shapes/intensities of $\Delta A_1$ to $\Delta C_1$ exhibits some changes at $x=0.4$ and 0.7 (marked by arrow bars), which is consistent with previous observation of a phase transition from tetragonal to cubic at $x=0.4$ and then to orthorhombic at $x=0.7$.[9]

The ranges of $\Delta A_1$ (from $\sim 529.0$ to 531.4 eV), $\Delta C_1$ (from $\sim 533.4$ to 535.8 eV), $\Delta B_1$ (from $\sim 531.4$ to 533.4 eV), and $\Delta D_1$ (from $\sim 535.8$ to 539.8 eV) are attributable to O $2p$–Ti $t_{2g}$, O $2p$–Ti $e_g$, O $2p$–Pb $6p$, and O $2p$–Ca $3d$ antibonding orbitals. The dependence of the O–Ti, O–Pb, and O–Ca hybridization on the Ca concentration can be estimated qualitatively from Fig. 4, which presents the integrated areas of $\Delta A_1 + \Delta C_1$, $\Delta B_1$, and $\Delta D_1$. The decrease of the $\Delta B_1$ area and the increase of the $\Delta D_1$ area with the increase of $x$ are approximately linear. In contrast, the variation of the $\Delta A_1 + \Delta C_1$ area can be roughly separated into three regions, which suggests that the structural transitions of PC$_x$TO are correlated primarily with the O–Ti hybridization. Figure 4 shows that the substitution of the A cation, Pb, by Ca not only decreases the O $2p$–Pb $6p$ but also O $2p$–Ti $3d$ hybridization. Ca has a smaller electronegativity than other two cations, Pb and Ti (1.0 vs 2.33 and 1.54, respectively).[14]
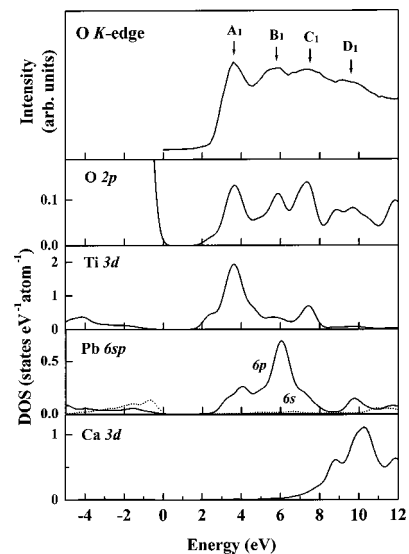


FIG. 2. The O $K$-edge XANES spectrum (upper solid-line) and the calculated O $2p$-, Ti $3d$-, Pb $6sp$-, and Ca $3d$-derived states for Pb$_{0.5}$Ca$_{0.5}$TiO$_3$. The first O $K$-edge feature has been aligned with that of the calculated O $2p$-derived states. Zero energy is the Fermi level.

Thus, electron charge is transferred from the Ca cation to both Pb and Ti cations in PC$_x$TO, which reduces the positive effective charges on Pb and Ti ions. Thus, the attractive Coulomb potentials at the Pb and Ti sites are reduced, which raises Pb and Ti orbital energies and reduces both O $2p$–Pb $6p$ and O $2p$–Ti $3d$ hybridization.

Earlier theoretical calculations suggested that the ferroelectric transition occur as a result of a balance between the long-range Coulomb interaction and the short-range force.[3] Zhong *et al.* also discussed the correlation between Coulomb interaction and the ferroelectric states[15] and argued that the Coulomb interaction leads to the splitting of LO and TO ferroelectric phonon modes. In recent studies of Pb-based PC$_x$TO[9] and Pb$_{1-x}$Sr$_x$TiO$_3$,[16] Kuo *et al.* reported that the frequency difference between LO and TO modes decreases when PC$_x$TO and Pb$_{1-x}$Sr$_x$TiO$_3$ transit from the tetragonal structure to the high-symmetry cubic structure. Kuo *et al.* interpreted their results as related to the reduction of long-range Coulomb interactions by enhanced Pb–O covalent bonding. However, based on present O $K$-edge results, it is argued in the following that the softening of the TO mode is not due to the enhanced Pb–O covalent bonding, but due to the reduction of Ti–O hybridization and Ti effective charge. The vibration frequency of the TO phonon mode is proportional to the square root of the force constant between cations and anions, which contains contributions from the attractive electrostatic Coulomb energies and hybridization. If the TO mode is contributed dominantly by the force constant between O and A cations, i.e., Pb and Ca, the TO mode will not soften by the substitution of Pb by Ca because Ca has a larger effective charge and enhanced Ca–O hybridization. Thus, the observed decrease of the LO–TO splitting suggests that the TO mode be contributed dominantly by the force constant between O and B cations, i.e., Ti ions. This argument is consistent with the understanding that ferroelectricity in PTO is due to the off-center displacement of B cation, Ti.

Figure 5 displays the Ti $L_{3,2}$-edge XANES spectra of PC$_x$TO. These spectra are split into $L_3$ and $L_2$ regions by the
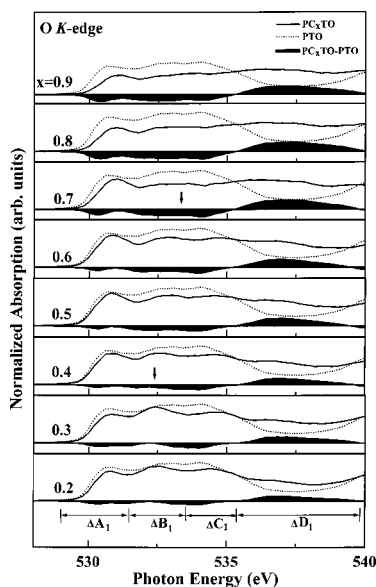
FIG. 3. The O $K$-edge XANES difference intensity curves between PC$_x$TO and PTO.



FIG. 5. Normalized Ti $L_{3,2}$-edge XANES spectra of PC$_x$TO. The dashed lines represent two best-fitted arctangent functions of the continuum step centered at the maximum height. The inset shows the magnified A$_2$ and B$_2$ features after the background subtraction.

spin-orbit interaction and each region contains $t_{2g}$ and $e_g$ splitting by approximately 2 eV due to the crystal-field effect. In these spectra, features A$_2$ and B$_2$ (C$_2$ and D$_2$) correspond to the $L_3$ ($L_2$) edge with $t_{2g}$ and $e_g$ symmetries, respectively.[17,18] Feature B$_2$ has a splitting of about 0.5 eV (indicated by vertical lines) for PC$_x$TO for $x$ between 0 and 0.3. The inset in Fig. 5 highlights the splitting by subtracting the background using two arctangent functions shown by the dashed lines. Feature B$_2$ is contributed by Ti $3d$ $e_g$ subband, which contains $3d_{x^2-y^2}$ and $3d_{z^2}$ orbitals. Since $3d_{x^2-y^2}$ and $3d_{z^2}$ orbitals point to the four side-corner and the two apex O ions of the octahedron, respectively, the variation of the Ti–O bond lengths due to Ti off-center displacement cause the splitting of feature B$_2$. In contrast, the $3d_{xy}$, $3d_{yz}$, and $3d_{zx}$ orbitals of the $t_{2g}$ subband point in directions between O ions, so that feature A$_2$ is not affected. The lack of splitting of feature D$_2$ may be due to the broadening of this higher energy feature. The similar splitting of 0.5 eV of the $e_g$ subband for $x = 0-0.3$ suggests that the Ti off-center displacement persists up to between $x = 0.3$ and 0.4. When $x = 0.4$ and larger, the splitting of feature B$_2$ disappears, which suggests the restoration of the Ti ion to the center of the
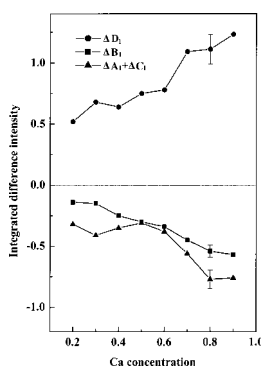
octahedron. The Ti $L_{3,2}$-edge XANES results suggest that the ferroelectric property in PC$_x$TO persists only up to a Ca concentration between 0.3 and 0.4.

FIG. 4. Integrated difference intensity curves, over $\Delta A_1 + \Delta C_1$, $\Delta B_1$, and $\Delta D_1$ regions vs the Ca concentration.
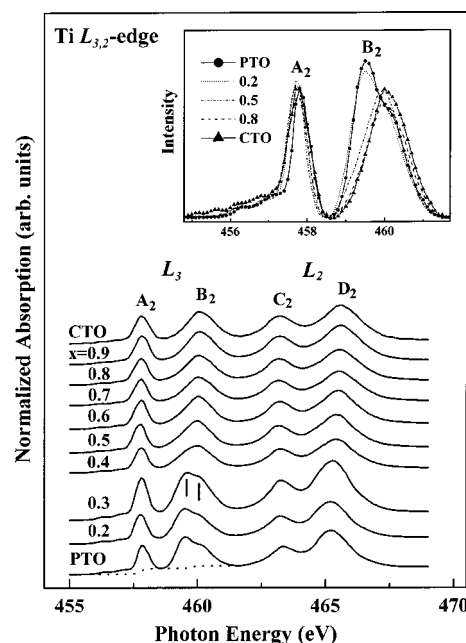
[1] For example, see M. E. Lines and A. M. Glass, *Principles and Applications of Ferroelectrics and Related Materials* (Clarendon, Oxford, 1979); J. F. Scott and C. A-Paz de Araujo, Science (Washington, DC, U.S.) **246**, 1400 (1989).

[2] C. Kittel, *Introduction to Solid State Physics*, 7th ed. (Wiley, New York, 1996).

[3] R. E. Cohen, Nature (London) **358**, 136 (1992).

[4] Y. Kuroiwa, S. Aoyagi, A. Sawada, J. Harada, E. Nishibori, M. Takata, and M. Sakata, Phys. Rev. Lett. **87**, 217601 (2001).

[5] K. Miura and M. Tanaka, Jpn. J. Appl. Phys., Part 1 **35**, 3488 (1996); H. Miyazawa, E. Natori, S. Miyashita, T. Shimoda, F. Ishii, and T. Oguchi, *ibid.* **39**, 5679 (2000).

[6] B. Ravel, Ph.D. thesis, University of Washington, 1997.

[7] K. Okazaki, Ferroelectrics **41**, 77 (1981).

[8] F. M. Pontes, D. S. L. Pontes, E. R. Leite, E. Longo, E. M. S. Santos, S. Mergulhã, A. Chiquito, P. S. Pizani, F. Lanciotti, Jr., T. M. Boschi, and J. A. Varela, J. Appl. Phys. **91**, 6650 (2002).

[9] S. Y. Kuo *et al.* (unpublished).

[10] H. C. Hsueh *et al.* (unpublished).

[11] M. C. Payne, M. P. Teter, D. C. Allen, T. A. Arias, and J. D. Joannopoulos, Rev. Mod. Phys. **64**, 1045 (1992).

[12] K. Asokan, J. C. Jan, J. W. Chiou, W. F. Pong, M.-H. Tsai, H. L. Shih, H. Y. Chen, H. C. Hsueh, C. C. Chuang, Y. K. Chang, Y. Y. Chen, and I. N. Lin, J. Phys.: Condens. Matter **13**, 11087 (2001).

[13] F. M. F. de Groot, M. Grioni, J. C. Fuggle, J. Ghijsen, G. A. Sawatzky, and H. Petersen, Phys. Rev. B **40**, 5715 (1989); **48**, 2074 (1993).

[14] *Table of Periodic Properties of the Elements* (Sargent-Welch Scientific, Skokie, IL, 1980).

[15] W. Zhong, R. D. King-Smith, and D. Vanderbilt, Phys. Rev. Lett. **72**, 3618 (1994).

[16] S. Y. Kuo, C. T. Li, and W. F. Hsieh, Appl. Phys. Lett. **81**, 3019 (2002).

[17] G. van der Laan, Phys. Rev. B **41**, 12366 (1990).

[18] F. M. F. de Groot, J. C. Fuggle, B. T. Thole, and G. A. Sawatzky, Phys. Rev. B **41**, 928 (1990).